



# Hierarchically Compartmentalized Supramolecular Gels through Multilevel Self-Sorting

Yiming Wang,<sup>†</sup> Matija Lovrak,<sup>†</sup> Qian Liu,<sup>†</sup> Chandan Maity,<sup>†,||</sup> Vincent A. A. le Sage,<sup>†</sup> Xuhong Guo,<sup>‡,§</sup> Rienk Eelkema,<sup>†</sup> and Jan H. van Esch<sup>\*,†</sup>

<sup>†</sup>Department of Chemical Engineering, Delft University of Technology, van der Maasweg 9, 2629 HZ Delft, The Netherlands

<sup>‡</sup>State Key Laboratory of Chemical Engineering, School of Chemical Engineering, East China University of Science and Technology, Shanghai 200237, China

<sup>§</sup>Engineering Research Center of Materials Chemical Engineering of Xinjiang Bingtuan, Shihezi University, Xinjiang 832000, China

## Supporting Information

**ABSTRACT:** Hierarchical compartmentalization through the bottom-up approach is ubiquitous in living cells but remains a formidable task in synthetic systems. Here we report on hierarchically compartmentalized supramolecular gels that are spontaneously formed by multilevel self-sorting. Two types of molecular gelators are formed in situ from nonassembling building blocks and self-assemble into distinct gel fibers through a kinetic self-sorting process; interestingly, these distinct fibers further self-sort into separated microdomains, leading to microscale compartmentalized gel networks. Such spontaneously multilevel self-sorting systems provide a “bottom-up” approach toward hierarchically structured functional materials and may play a role in intracellular organization.

The archetype example of a compartmentalized system is the living cell,<sup>1</sup> in which hierarchical compartmentalization at the level of organelles, followed by their intracellular organization, enables complex physiological functions.<sup>2</sup> Interestingly, the spatial organization and functions of cells are entirely created through the self-assembly of multicomponent biological subunits. Although the self-sorting of these different components into biological supramolecular structures is well known, the processes that lead to higher-level organization of these structures into different compartments remain poorly understood. To mimic the intracellular compartmentalization can not only improve our understanding of the intracellular scenario but also inspire the design and construction of hierarchically compartmentalized functional objects,<sup>3</sup> such as artificial cells<sup>4</sup> and microreactors.<sup>5</sup>

In recent years, much progress has been made toward the development and understanding of multicomponent self-assembly in synthetic systems.<sup>6</sup> In particular, self-sorting or orthogonal self-assembly, that is, the independent self-assembly of different building blocks into distinct supramolecular structures,<sup>7</sup> is a viable route toward complex systems composed of different coexisting supramolecular structures, such as fibers,<sup>8</sup> micelles or vesicles,<sup>9</sup> and liquid crystals.<sup>10</sup> Despite these advances, self-sorting in synthetic systems is still limited to the molecular level, and multilevel organization

toward hierarchical supramolecular architectures remains an elusive goal.

Here we present a rare example of hierarchical compartmentalization on both nanoscale and microscale that has resulted exclusively by the self-assembly of different synthetic molecules. We find that molecular gelators bearing a common self-assembling motif first self-sort into distinct nanofibers, which further self-sort into separated microdomains, resulting in hierarchically compartmentalized supramolecular gels. Our findings suggest that subtle variations in interactions can also enable self-sorting. Importantly, such hierarchically compartmentalized systems are formed spontaneously, without consumption of fuels, thereby contributing to our understanding of self-sorting and compartmentalization in both synthetic and natural systems.

In this work, we used a modular supramolecular gel system with tunable properties based on the in situ formation of tris-hydrazone gelators from soluble hydrazide (**H**) and aldehydes.<sup>11</sup> By combining an anionic (**A**<sup>−</sup>) and a neutral aldehyde (**A**), we obtained a multicomponent gelator system consisting of neutral (**NGs**: **HA**<sub>3</sub>) and charged gelators (**CGs**: **HA**<sub>2</sub>**A**<sup>−</sup>, **HAA**<sub>2</sub><sup>−</sup>, and **HA**<sub>3</sub><sup>−</sup>) (Figure 1a). We anticipated that the introduction of charges may prevent bundling, thereby influencing the viscoelastic properties of the gels.<sup>11,12</sup>

In this study, unless otherwise mentioned, the samples were prepared from a mixture of **H** (20 mM) and aldehydes **A**, **A**<sup>−</sup> (120 mM, different mol % **A**<sup>−</sup>) dissolved in a phosphate buffer (0.1 M, pH 7.0). The total concentration of aldehydes was constantly kept six times higher than **H** to achieve full conversion of **H** into tris-hydrazone products. In a typical experiment, a gelator precursor solution including 30 mol % **A**<sup>−</sup> was prepared. After 24 h, a turbid gel was formed, as determined by tube inversion test (Figure 1b). Surprisingly, confocal laser scanning microscopy (CLSM) revealed that the resulting gel consisted of worm-like microstructures (Figure 1c,d), which are very different from the typical fibrous networks of **HA**<sub>3</sub> gel (Figure S1) and other supramolecular gels.<sup>11,13</sup> Three dimensional (3D) CLSM revealed that the gels consisted of closely packed crumpled sheets (Figure 1e and Movie S1), and the worm-like structures appeared to be 2D

Received: October 3, 2018

Published: December 18, 2018



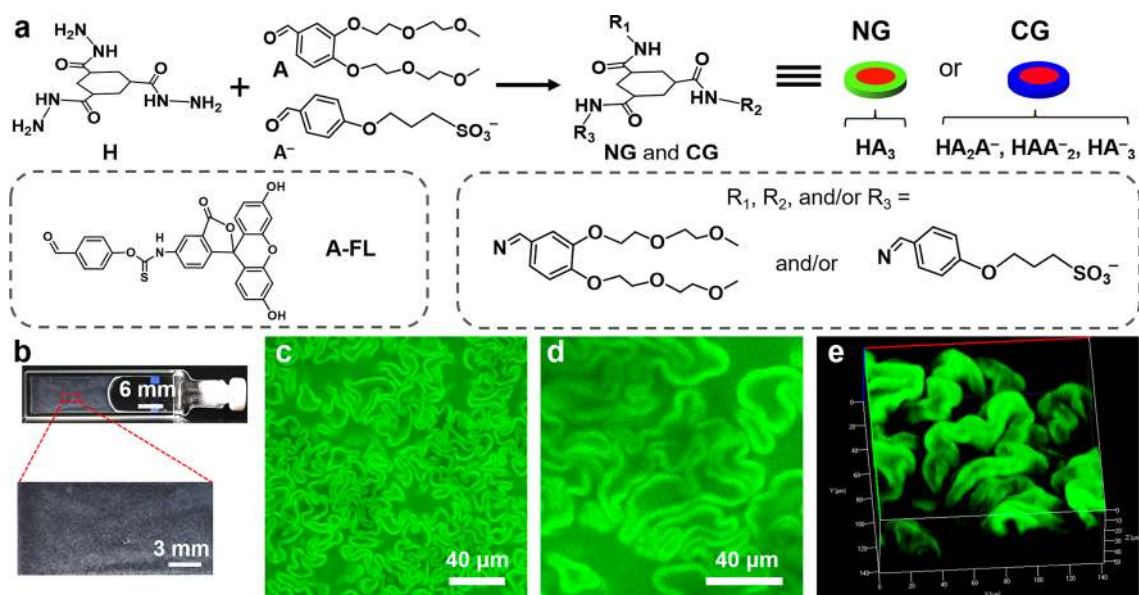


**Figure 1.** (a) Schematic of formation of gelators from the precursors of H, A, and A<sup>-</sup>. A-FL was used as a fluorescence label for self-assembled structures. (b) Photograph of the gel sample. (c) CLSM image of the gel networks. (d) Magnified 2D and (e) the corresponding 3D CLSM images (transparent mode) of the gel networks. (c–e) 30 μM A-FL was added to the pregel solution.

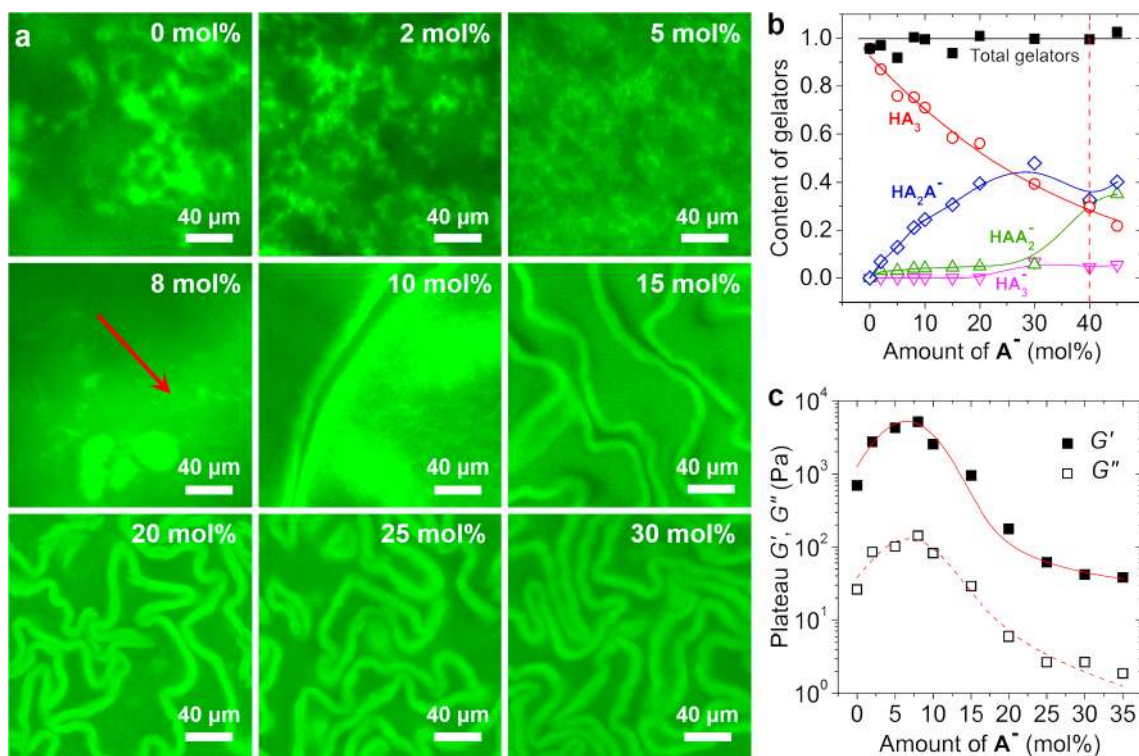


**Figure 2.** (a) CLSM images of the gel networks formed with different mol % A<sup>-</sup>. (b) Gelator composition of the gels, the amount was normalized by the initial concentration of H. (c) Influences of mol % A<sup>-</sup> on the gel stiffness. 30 μM A-FL was added for CLSM tests.

cross sections of these sheets. Notably, these unique networks were independent of the addition of the probe A-FL (Figure S2).

To investigate whether the appearance of the crumpled sheets is caused by the presence of A<sup>-</sup>, we varied the amount of A<sup>-</sup> and explored its effects on the gel morphology (Figure 2a and Figure S3). We found that gels were formed only if <40 mol % A<sup>-</sup> was added. Furthermore, the addition of small amounts of A<sup>-</sup> already led to a marked decrease in the cluster

sizes (Figure 2a, 0 to 5 mol %). Interestingly, at 8 mol % A<sup>-</sup>, some isolated structures were formed (arrowed area in Figure 2a), and further increasing the amount of A<sup>-</sup> led to crumpled sheets. Importantly, the density of the crumpled sheets increases with the amount of A<sup>-</sup>, indicating that the sheet structure is related to the charged species. High-performance liquid chromatography (HPLC) analysis confirmed that the gels consisted of two types of gelators, that is, NGs and CGs, as was expected (Figure 2b and Figure S4).<sup>11a</sup> In each sample,

H was fully converted to tris-hydrazone gelators, and the amount of CGs was increased with mol % A<sup>-</sup>. This confirms the aforementioned correlation between the crumpled sheets and CGs. When the added A<sup>-</sup> was >40 mol %, the molar fraction of CGs was exceeded 0.75. Most likely, these high concentrations of CGs hinder either the self-assembly of gelators or the cross-linking of fibers because of the electrostatic repulsion, with both scenarios explaining the lack of gel formation in samples with >40 mol % A<sup>-</sup>.

After studying the gel structures, we applied oscillatory rheology to investigate the effects of the content of A<sup>-</sup> on the viscoelastic properties of the gels (Figure 2c and Figure S5). We found that the addition of small amounts of A<sup>-</sup> from 0 up to 8 mol % led to an increase in  $G'$  from ~700 Pa to 5.0 kPa, but larger mol % A<sup>-</sup> caused a dramatic decrease in  $G'$ , from ~5.0 kPa (8 mol % A<sup>-</sup>) to ~40 Pa (35 mol % A<sup>-</sup>). In all of these samples,  $G'$  is constantly higher than  $G''$ , indicating the gel state. This  $G'$  maximum at 8 mol % A<sup>-</sup> coincides with the initial reduction of cluster sizes, followed by the appearance of crumpled sheets, as observed in the CLSM tests. Apparently, the reduction in cluster sizes leads to an increase in gel stiffness, whereas the formation of crumpled sheets weakens the gels.

In the subsequent experiments, we are keen to unveil how these gel networks can be formed. Closer inspection of the gel networks by CLSM revealed that the areas in between the sheets displayed typical fibrous networks (right top, Figure 3a),

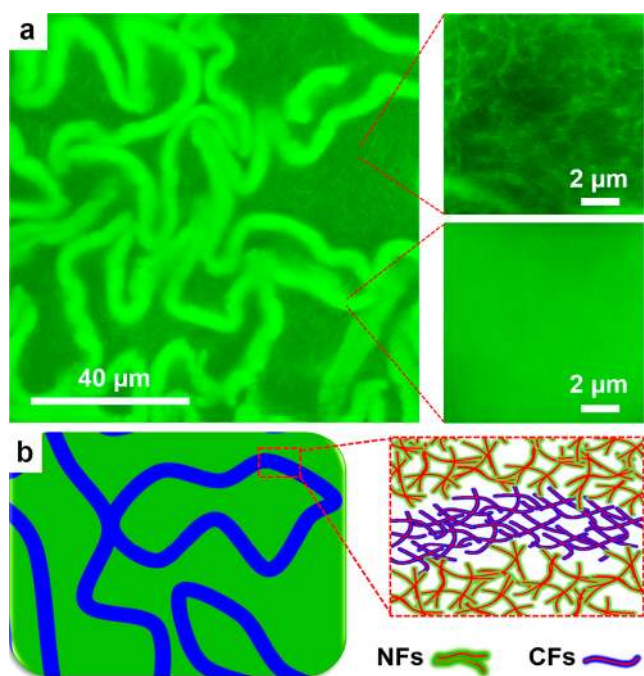


**Figure 3.** (a) Morphologies of the gel networks (30 mol % A<sup>-</sup>, 30 μM A-FL) in crumpled sheets and the areas in between the sheets. (b) Illustrated composition of the gel networks.

similar to the morphology of HA<sub>3</sub> gels,<sup>11a</sup> whereas the crumpled sheets showed uniform fluorescence without any visible fibrous structures (right bottom, Figure 3a). Bleaching experiments revealed that the fluorescence recovered slowly, indicating the cross-linked state in both areas (Figure S6). Cryo-TEM confirmed that the gels are composed of thin fibers and fibrous bundles (Figure S7). Moreover, polarized light

microscopy showed that neither the crumpled sheets nor the fibrous networks are birefringent (Figure S8). We therefore conclude that the coarse network consists of randomly oriented fibrous bundles that are visible by CLSM, whereas the crumpled sheets consist of randomly dispersed finer fibers that cannot be resolved by optical microscopy.

We were wondering how these different fibrous networks are related to the composition of the gelators. Clearly, the appearance of the crumpled sheets is related to A<sup>-</sup>, whereas the coarse networks are more prominent at lower A<sup>-</sup> (Figure 2a). Therefore, it seems likely that the coarse networks are composed of neutral fibers (NFs) formed from NGs, as they are prone to form bundles (Figure S1).<sup>11a,14</sup> In contrast, the finer fibers in the crumpled sheets are charged fibers (CFs) containing at least a significant fraction of CGs, which can effectively prevent bundling relying on the interfibrillar electrostatic repulsion (Figure 3b). Most interestingly, the formation of different fibers and their subsequent organization into different microdomains starting from a mixture of gelator molecules would involve the self-sorting of the gelators first at the supramolecular level and subsequently at the macroscopic level.

To investigate the above hypothesis, we first investigated the distribution of CFs in the gel networks using CLSM by selectively staining the CFs with a cationic dye Hoechst 33342 (blue, Figure S9). Simultaneously A-FL (green) was used to stain all fibers. CLSM showed again in the green channel the gel networks with crumpled sheets, indicating that the presence of Hoechst 33342 does not affect the gel morphology (Figure 4a). However, in the blue channel, only the crumpled sheets appeared to be stained by Hoechst 33342 (Figure 4a, Figure S3, and Movie S2). Additionally, HA<sub>3</sub> gel was not stained by Hoechst 33342 (Figure S10), indicating no appreciable interactions between NFs and Hoechst 33342. These results unambiguously confirm that the crumpled sheets consist of CFs, whereas the coarse networks are formed by NFs.

To investigate how self-sorting of a molecular mixture leads to different microdomains, we monitored the formation of these gel networks over time by CLSM and rheology while analyzing the molecular composition over time by HPLC. HPLC experiments showed that both A and A<sup>-</sup> reacted with H at similar rates and complete conversion within 5 h (Figure S11), in line with a previous study.<sup>11a</sup> This result confirms that the proposed self-sorting of NGs and CGs is not simply due to their different formation rates. Rheological measurements showed that after ~40 min to ~4.3 h, depending on the amount of A<sup>-</sup>,  $G'$  started to rise, indicating the onset of fiber formation (Figure 4c and Figure S5), and then gradually increased until reaching the final strengths.

Then, we followed the formation of the gel networks over time using CLSM by labeling the samples with A-FL and Hoechst 33342 (Figure 4b and Movie S3). Initially the sample only displayed green fluorescence; however, after ~1.3 to ~4.9 h, depending on the amount of A<sup>-</sup>, a homogeneous blue fluorescence started to appear (Figure 4b,c). We assign the development of the blue fluorescence to the formation of CFs, and, interestingly, its development is markedly delayed compared with the onset of fiber formation observed by rheology. Apparently, the onset of fiber formation observed by rheology marks the formation of NFs, which precedes the formation of CFs. The CLSM experiments showed that over the next 2 h the blue fluorescence gradually increased but remained homogeneous. However, after ~5 h, the blue

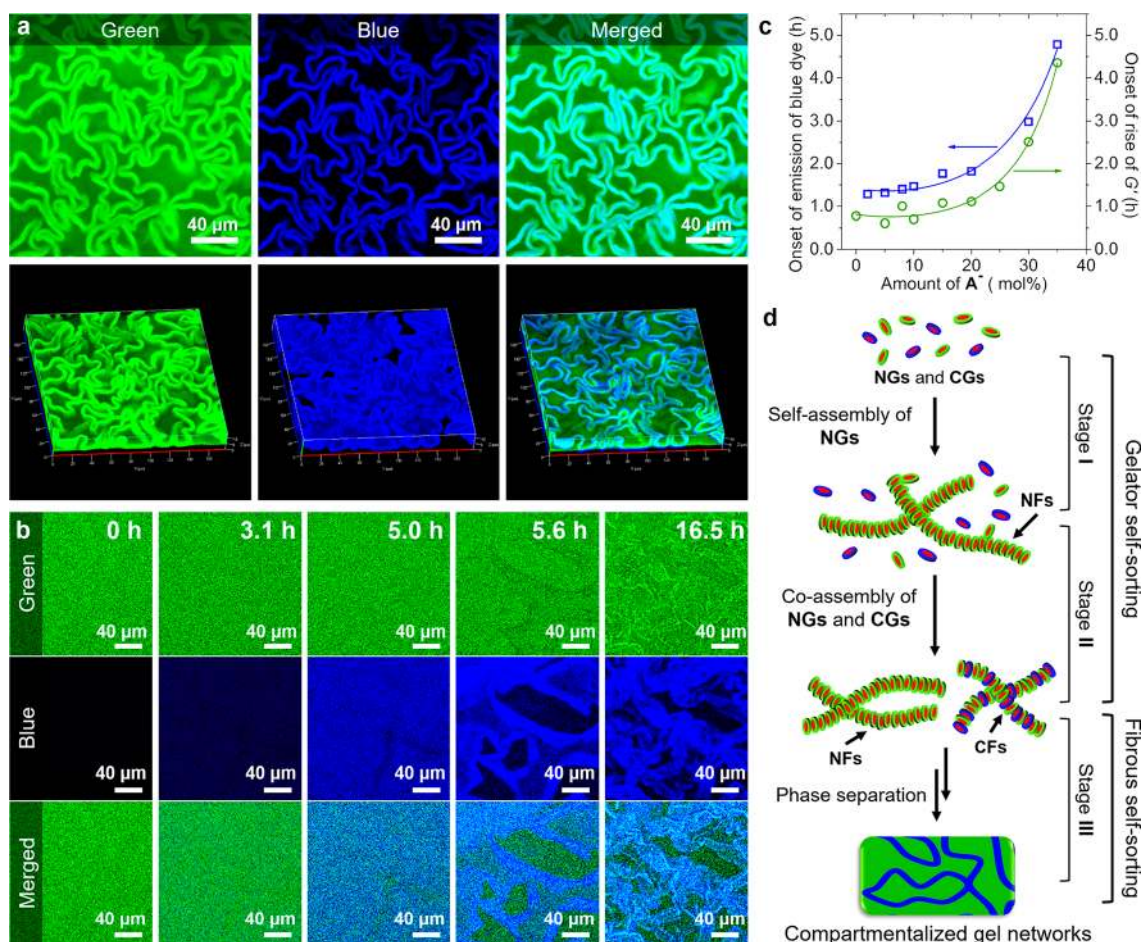


**Figure 4.** (a) Split 2D (top) and the corresponding 3D (bottom) CLSM images. (b) Formation process of the gel networks (30 mol %  $A^-$ ). (c) Critical formation time of fibers as a function of mol %  $A^-$ . (d) Illustration of the multilevel self-sorting process. 30  $\mu\text{M}$  A-FL and 20  $\mu\text{M}$  Hoechst 33342 were added for CLSM tests.

fluorescence became inhomogeneous, and after  $\sim 5.6$  h blue-stained sheet structures became visible and separated from the bulk area, gradually collapsing into a crumpled state. A control sample without Hoechst 33342 gave rise to the same gel-formation process (Figure S12 and Movie S4), indicating the lack of impact of the addition of Hoechst 33342 on the gel formation process.

Altogether, these results clearly reveal that the formation of the gel networks with crumpled sheets proceeds through three stages (Figure 4d). In stage I, characterized by a rise of  $G'$  and the absence of blue fluorescence, NFs are formed through self-assembly of NGs. In stage II, marked by the development of a homogeneous blue fluorescence, CFs are formed and remain homogeneously mixed with NFs. Most likely, the delayed formation of CFs compared with NFs is related to a higher critical assembly concentration (CAC) of CGs compared with NGs, caused by electrostatic repulsions (Figures S13 and S14). Whereas NGs and CGs are formed at the same rate, NGs reach their CAC prior to CGs, and as a result, NFs are formed earlier in time than CFs, thereby providing an example of kinetic self-sorting.<sup>6a,15</sup> Finally, in stage III, characterized by macroscopic phase separation, a higher-level self-sorting takes place, in which NFs and CFs separate into different microdomains consisting of coarse networks of NFs and crumpled sheets of CFs, respectively. Although the mechanism of this second self-sorting process remains unclear, it should

also be noted that in aqueous two-phase systems, polyethylene glycol (PEG) polymers and anionic polyelectrolytes are prone to form separated phases.<sup>16</sup>

In summary, we have shown how multilevel self-sorting processes can lead to the spontaneous formation of hierarchically compartmentalized supramolecular gels. This finding would accelerate our understanding of both the natural and synthetic self-sorting systems and can serve as a starting point for the “bottom-up” fabrication of hierarchically compartmentalized structures for applications in, for example, synthetic biology,<sup>4</sup> catalysis,<sup>17</sup> and drug delivery.<sup>18</sup>

## ■ ASSOCIATED CONTENT

### 📄 Supporting Information

The Supporting Information is available free of charge on the ACS Publications website at DOI: 10.1021/jacs.8b09596.

Experimental procedures and supporting figures (PDF)

Movie S1 (AVI)

Movie S2 (AVI)

Movie S3 (AVI)

Movie S4 (AVI)

## ■ AUTHOR INFORMATION

### Corresponding Author

\*j.h.vanesch@tudelft.nl.

ORCID 

Yiming Wang: 0000-0002-8269-8304

Xuhong Guo: 0000-0002-1792-8564

Rienk Eelkema: 0000-0002-2626-6371

Jan H. van Esch: 0000-0001-6116-4808

## Present Address

<sup>||</sup>C.M.: School of Chemical Engineering and Physical Science, Lovely Professional University, Punjab, India.

## Notes

The authors declare no competing financial interest.

## ■ ACKNOWLEDGMENTS

We gratefully acknowledge the China Scholarship Council and The Netherlands Organization for Scientific Research (NWO VIDI) for financial support.

## ■ REFERENCES

- (1) Hurlley, S. *Science* **2009**, *326*, 1205.
- (2) (a) Brangwynne, C. P.; Tompa, P.; Pappu, R. V. *Nat. Phys.* **2015**, *11*, 899. (b) Devos, D. P.; Graf, R.; Field, M. C. *Curr. Opin. Cell Biol.* **2014**, *28*, 8. (c) Nott, T. J.; Petsalaki, E.; Farber, P.; Jervis, D.; Fussner, E.; Plochowietz, A.; Craggs, T. D.; Bazett-Jones, D. P.; Pawson, T.; Forman-Kay, J. D.; Baldwin, A. J. *Mol. Cell* **2015**, *57*, 936.
- (3) (a) Ahmed, R.; Patra, S. K.; Chabanne, L.; Faul, C. F. J.; Manners, I. *Macromolecules* **2011**, *44*, 9324. (b) Faul, C. F. J. *Acc. Chem. Res.* **2014**, *47*, 3428.
- (4) (a) Deng, N. N.; Yelleswarapu, M.; Zheng, L.; Huck, W. T. J. *Am. Chem. Soc.* **2017**, *139*, 587. (b) Weiss, M.; Frohnmayer, J. P.; Benk, L. T.; Haller, B.; Janiesch, J. W.; Heitkamp, T.; Borsch, M.; Lira, R. B.; Dimova, R.; Lipowsky, R.; Bodenschatz, E.; Baret, J. C.; Vidakovic-Koch, T.; Sundmacher, K.; Platzman, I.; Spatz, J. P. *Nat. Mater.* **2017**, *17*, 89.
- (5) Hosta-Rigau, L.; Shimoni, O.; Stadler, B.; Caruso, F. *Small* **2013**, *9*, 3573.
- (6) (a) Safont-Sempere, M. M.; Fernandez, G.; Wurthner, F. *Chem. Rev.* **2011**, *111*, 5784. (b) Kumar, D. K.; Steed, J. W. *Chem. Soc. Rev.* **2014**, *43*, 2080.
- (7) (a) Kato, T. *Science* **2002**, *295*, 2414. (b) Heeres, A.; van der Pol, C.; Stuart, M.; Friggeri, A.; Feringa, B. L.; van Esch, J. *J. Am. Chem. Soc.* **2003**, *125*, 14252.
- (8) (a) Cornwell, D. J.; Daubney, O. J.; Smith, D. K. *J. Am. Chem. Soc.* **2015**, *137*, 15486. (b) Moffat, J. R.; Smith, D. K. *Chem. Commun.* **2009**, 316. (c) Colquhoun, C.; Draper, E. R.; Eden, E. G. B.; Cattoz, B. N.; Morris, K. L.; Chen, L.; McDonald, T. O.; Terry, A. E.; Griffiths, P. C.; Serpell, L. C.; Adams, D. J. *Nanoscale* **2014**, *6*, 13719. (d) Draper, E. R.; Eden, E. G.; McDonald, T. O.; Adams, D. J. *Nat. Chem.* **2015**, *7*, 848. (e) Singh, N.; Zhang, K.; Angulo-Pachon, C. A.; Mendes, E.; van Esch, J. H.; Escuder, B. *Chem. Sci.* **2016**, *7*, 5568.
- (9) (a) Brizard, A.; Stuart, M.; van Bommel, K.; Friggeri, A.; de Jong, M.; van Esch, J. *Angew. Chem., Int. Ed.* **2008**, *47*, 2063. (b) Boekhoven, J.; Brizard, A. M.; Stuart, M. C. A.; Florusse, L.; Raffy, G.; Del Guerzo, A.; van Esch, J. H. *Chem. Sci.* **2016**, *7*, 6021. (c) Vieira, V. M. P.; Hay, L. L.; Smith, D. K. *Chem. Sci.* **2017**, *8*, 6981.
- (10) Kato, T.; Hirai, Y.; Nakaso, S.; Moriyama, M. *Chem. Soc. Rev.* **2007**, *36*, 1857.
- (11) (a) Boekhoven, J.; Poolman, J. M.; Maity, C.; Li, F.; van der Mee, L.; Minkenberg, C. B.; Mendes, E.; van Esch, J. H.; Eelkema, R. *Nat. Chem.* **2013**, *5*, 433. (b) Poolman, J. M.; Boekhoven, J.; Besselink, A.; Olive, A. G.; van Esch, J. H.; Eelkema, R. *Nat. Protoc.* **2014**, *9*, 977. (c) Poolman, J. M.; Maity, C.; Boekhoven, J.; van der Mee, L.; le Sage, V. A. A.; Groenewold, G. J. M.; van Kasteren, S. I.; Versluis, F.; van Esch, J. H.; Eelkema, R. *J. Mater. Chem. B* **2016**, *4*, 852.
- (12) Martin, A. D.; Wojciechowski, J. P.; Robinson, A. B.; Heu, C.; Garvey, C. J.; Ratcliffe, J.; Waddington, L. J.; Gardiner, J.; Thordarson, P. *Sci. Rep.* **2017**, *7*, 43947.
- (13) (a) Du, X.; Zhou, J.; Shi, J.; Xu, B. *Chem. Rev.* **2015**, *115*, 13165. (b) Draper, E. R.; Adams, D. J. *Chem.* **2017**, *3*, 390.
- (14) Wang, Y.; Versluis, F.; Oldenhof, S.; Lakshminarayanan, V.; Zhang, K.; Wang, Y.; Wang, J.; Eelkema, R.; Guo, X.; van Esch, J. H. *Adv. Mater.* **2018**, *30*, 1707408.
- (15) Raeburn, J.; Adams, D. J. *Chem. Commun.* **2015**, *51*, 5170.
- (16) Mace, C. R.; Akbulut, O.; Kumar, A. A.; Shapiro, N. D.; Derda, R.; Patton, M. R.; Whitesides, G. M. *J. Am. Chem. Soc.* **2012**, *134*, 9094.
- (17) (a) Shi, J. F.; Du, X. W.; Huang, Y. B.; Zhou, J.; Yuan, D.; Wu, D. D.; Zhang, Y.; Haburcak, R.; Epstein, I. R.; Xu, B. *J. Am. Chem. Soc.* **2015**, *137*, 26. (b) Tang, X. Y.; Huang, Z. H.; Chen, H.; Kang, Y. T.; Xu, J. F.; Zhang, X. *Angew. Chem., Int. Ed.* **2018**, *57*, 8545.
- (18) (a) Boekhoven, J.; Koot, M.; Wezendonk, T. A.; Eelkema, R.; van Esch, J. H. *J. Am. Chem. Soc.* **2012**, *134*, 12908. (b) Majumder, P.; Baxa, U.; Walsh, S. T. R.; Schneider, J. P. *Angew. Chem.* **2018**, *130*, 15260.